Identifying Robot Parameters Using Partial Pose Information

Ambarish Goswami, Arthur Quaid, and Michael Peshkin

The absolute accuracy of a robot depends to a large extent on the accuracy with which its kinematic parameters are known. Many methods have been explored for inferring the kinematic parameters of a robot from measurements taken as it moves. Some require an external global positioning system, usually optical or sonic. Instead, we have used a simple radial-distance linear transducer (LVDT) which measures the distance from several fixed points in the workspace to the robot's endpoint. This incomplete pose information (one dimensional rather than six dimensional) is accumulated as the robot endpoint is moved within one or more hemispherical "shells" centered about the fixed points. Optimal values for all of the independent kinematic parameters of the robot can then be found.

Here we discuss the motivation, theory, implementation, and performance of this particularly easy calibration and parameter identification method. We also address a recent disagreement in literature about the type of measuring system (in particular, the dimensionality of the pose measurements) needed to fully identify a robot's kinematic parameters.

Absolute Accuracy versus Repeatability

It is important to distinguish between the *absolute accuracy* and the *repeatability* of a robotic manipulator. Repeatability of a robot is the precision with which its endpoint achieves a particular pose (endpoint position and orientation) under repeated commands to the same set of joint angles. Gear backlash, and sensor and servo precision are some of the factors affecting robot repeatability.

Absolute accuracy is the closeness with which the robot's actual pose matches the pose predicted by its controller. A robot may have high repeatability while having low absolute accuracy. Given the joint angles, the controller of a robot computes its endpoint location and orientation. For this it needs an accurate description of the robot which involves many physical parameters such as link lengths and joint offset angles. These numerical parameters make up the kinematic model of the robot. The absolute accuracy of the robot depends on the accuracy of this model.

A high repeatability is of prime importance for a variety of robot applications such as pick and place, spray painting, and welding. In these operations a robot is guided through the required endpoint motions (with the help of a teach-pendant) and the corresponding joint-angles are recorded. During actual operation, the robot "plays back" the recorded joint angles.

Tasks involving off-line planning, on the other hand depend on the absolute accuracy of the robot. For us, accuracy issues arose in the context of employing a robotic system as a precision positioning device in a medical operating room [15], [27]. In this application, a robot may improve the quality of orthopedic surgery by accurately guiding a surgeon's saw. Cutting angles are selected on the basis of measured anatomical features (e.g., bone dimensions) obtained through preoperative CT scans. Robot accuracy is required so that the cuts performed are at the same location and angle as the ones planned.

For various reasons, the numerical values of the kinematic parameters for a robot may not be correct. This may be due to manufacturing tolerances, deviations such as link and joint compliance, or time-dependent effects such as gear wear and component damage. Therefore, the nominal kinematic model which is
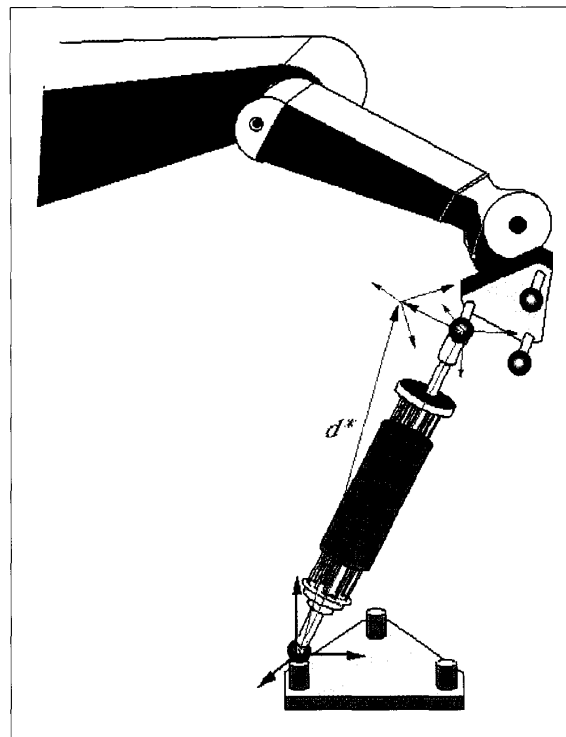

Fig. 1. The calibration system with the ball-bar connected between one of three steel spheres attached to the robot endpoint and a magnetic chuck mounted on the table.

programmed into the robot's controller does not accurately predict the endpoint pose from the joint angles.

To address this problem we may re-evaluate the numerical parameters of a robot's kinematic model by using a calibration scheme. Robot calibration typically involves externally measuring the pose (position and orientation) of a robot's endpoint at different commanded locations in the robot's workspace. The measured coordinates are compared to those predicted by the robot's controller, which are based on the existing kinematic model and the measured robot joint angles. The difference between the actual (measured) coordinates and the predicted ones is the error. The existing kinematic model is then replaced by a new "optimal" model which minimizes the aggregate error.

Many robot calibration techniques have been reported in the literature. These techniques differ in the hardware employed for external measurements, the type of collected data (position data, orientation data, etc.) and in the nature of the optimization algorithm that generates new kinematic parameters. Among the most popular measurement systems are theodolites, lasers, sonic digitizers, proximity sensors, and three-cable measuring systems. (See [16] for a description of common measurement devices.) The selection of a particular measurement system is based upon criteria such as cost, ease of use, set-up time, accuracy of measurements, and volume of calibrated workspace.

Scope and Contribution

Robot calibration, in its broadest scope, addresses static errors (such as those caused by changes in link dimensions, gear wear, elastic bending of links, etc.) as well as dynamic errors (such as those caused by vibration) [21]. The static errors of a manipulator may result from geometric errors as well as from non-geometric errors. Geometric errors are related to link dimensions and joint encoder characteristics. The non-geometric errors are caused by effects such as gear train compliance, motor bearing wobble, and gear backlash. The method described in this paper corrects the static geometrical errors of a robot by reevaluating its kinematic parameters only. With a suitable model, our approach also could be extended to include non-geometric parameters. Since typically 90% of the RMS endpoint positioning error is caused by errors in the static geometric parameters [14], the additional improvement in robot accuracy resulting from the compensation of non-geometric parameter errors will be smaller.

The measuring device we used is a *telescopic ball-bar system* manufactured by Automated Precision, Inc. It is relatively inexpensive, easy to use, and highly accurate [16], [26]. The heart of the system is a linear transducer (LVDT), with a maximum travel of 7.5 cm. The LVDT precisely measures the distance of the robot endpoint from a fixed location. The system setup is shown in Fig. 1.

The ball-bar has a magnetic chuck permanently mounted on one end, and a removable high precision steel sphere mounted at the opposite end. The removable sphere allows the insertion of extension rods, which permit the nominal length of the device to be increased to reach more of the robot's workspace if desired. Additional magnetic chucks and steel spheres mate with the ends of the device to form spherical joints. In our implementation, the sphere end of the ball-bar pivots around one of three stationary magnetic chucks mounted in the workspace, while the chuck end of the ball-bar mates with one of three steel spheres connected to the robot's moving endpoint.

The calibration system must read robot joint positions and LVDT lengths for various robot poses within the workspace of the robot and within the reach of the ball-bar. Simultaneously, using forward kinematics and the nominal robot kinematic model, the expected position of the robot endpoint can be calculated from the joint positions. This position gives us the expected location of the movable end of the ball-bar. The distance between the robot endpoint and the fixed end of the ball-bar is the expected ball-bar length. The difference between the expected ball-bar length and the actual length measured by the LVDT is the error due to incorrect robot kinematic parameters. We compute new parameters which minimize this error.

The maximum number of *independent* kinematic parameters [6]-[8], [12], N, of a robot is given by

$$N = 5n_r + 3n_p + 6 \qquad (1)$$

where n_r is the number of revolute joints and n_p is the number of prismatic joints in the robot. (In [6]-[8], equation (1) was given as $N = 4n_r + 2n_p + 6$ because a conversion constant for each joint encoder was not included in the kinematic model.)

Regardless of the total number of physical parameters in the kinematic description of the robot, which may be much larger, N is the maximum number of parameters that can be identified by collecting data at the robot's endpoint alone. N is also the number of parameters sufficient to compute the endpoint pose from the robot's joint angles.

A robot endpoint pose consists of endpoint position (three measurements) and orientation (three measurements) with respect to a base coordinate frame. In order to identify a complete set of N independent parameters of a robot, one might expect to need to measure the position and orientation of the robot endpoint, which would require the use of a sophisticated six degrees-of-freedom (DOF) measuring device. We show here that a simple measuring device, capable of collecting only partial pose information (just a radial distance), is equally effective in identifying all of the independent robot kinematic parameters. This represents an economic and easy route to robot calibration.

Choice of a kinematic model is important for calibration; we discuss the Sheth-Uicker model below. Next we describe the Levenberg-Marquardt algorithm which we have used for parameter optimization, on account of its robustness and its ability to handle singular systems. We then describe data collection and results. The final section contains a discussion of various sets of incomplete pose information, with regard to their sufficiency or insufficiency for complete parameter identification.

Kinematic Model

The endpoint pose (position and orientation) of a robot may be expressed as a nonlinear function of the physical link parameters and the joint encoder parameters, which are presumed to be constants, and of the measured joint revolute angles or prismatic displacements, which are, of course, variables. The former group, the constants, comprise the kinematic parameters we seek to identify.

Many kinematic models have been suggested. Reference [13] contains an overview of various kinematic models in use. One has to be particularly careful in selecting a kinematic model for calibration purposes. For instance, a model which is compact and efficient for forward and inverse kinematics may give rise to

numerical instability during parameter optimization. References [6] and [7] discuss desirable properties of a kinematic model.

For calibration, the two most important properties of a kinematic model are *completeness* and *proportionality* [6]. In a *complete* kinematic model every possible kinematic change of the robot will be reflected by the model parameters. If we use an incomplete model for calibration and parameter estimation, the errors in the unmodeled parameters will be partially corrected by adjustments of physically unrelated parameters. This results in an optimized parameter set that does not reflect the actual values of the robot's physical features, and may result in suboptimal robot accuracy.

Proportionality of a kinematic model requires that a small change in the physical features of a robot is reflected by only a small change in the model parameters. Proportionality is a similar concept to mathemetical *continuity* of the model parameters and ensures the numerical stability of the optimization process.

In this work we adopt the Sheth-Uicker kinematic model [1], [22], [23]. It is complete, proportional, and easy to assign to a manipulator. In this model three translational and three angular parameters (*ZYX*-ordered Euler angles) are used to describe the position and orientation of the distal coordinate frame relative to the proximal coordinate frame of a link. Zeigert and Datseris [28] point out the necessity of using a six-parameter kinematic model. There are other six-parameters models [2], [4], [24], and good overviews may be found in [13], [21], [28].

To model the joint encoder parameters we assume a linear relation between the output of an encoder and the actual joint angle. Following [1], [12], [23] we model a manipulator joint as

$$\theta = \theta_0 + kq \qquad (2)$$

where θ is the actual joint angle, θ_0 is the joint encoder zero-point offset, q is the encoder output, and k is the joint encoder transducer constant. An ideal optical encoder should have unity k.

A PUMA 560 manipulator, which we used in our experiment, is an open-loop six DOF kinematic chain composed of a base and an end-effector (which we may design) connected by five intermediate links and six joints. Allowing six parameters per link and two parameters per joint, a total of 54 parameters (for seven links and six joints) are required to completely describe the manipulator.

According to (1), only 36 of these parameters may be identified. As mentioned above, these 36 are a sufficient set to compute the endpoint pose from joint encoder outputs, even though they are not sufficient, for instance, to identify if the manufacturing tolerances have been exceeded. Our model therefore contains 18 extra parameters, which are called *redundant parameters* [12]. The resulting transformation matrix T relating the endpoint pose to the global coordinate frame may be expressed as a sequential multiplication of 13 local homogeneous transformation matrices (one for each of the seven links and six joints), as follows:

$$T = T_1^L T_1^J T_2^L T_2^J T_3^L \dots T_6^L T_6^J T_7^L , \qquad (3)$$

where T_i^L and T_i^J represent the link transformation matrices and the joint transformation matrices, respectively, of the ith link or joint. The global position and orientation of the endpoint can be easily extracted from the matrix T above [11]. We use the position components to calculate the expected length of the ball-bar: the distance from a robot endpoint-mounted steel sphere to the fixed magnetic chuck.

Optimization

In practice, the computed distance from an endpoint-mounted steel sphere to a fixed magnetic chuck will be different from the actual distance, as measured by the LVDT in the ball-bar. The difference, known as the *residual*, is determined at many data collection points scattered throughout the reachable workspace. The aggregate sum-of-squares of the residuals over n data collection points ϕ is calculated as

$$\phi = \sum_{i=1}^{n}(d^*(i) - d_c(i))^2 , \qquad (4)$$

where $d^*(i)$ and $d_c(i)$ are the measured distance and the computed distance, respectively, at the ith data collection point. The quantity ϕ is used as an objective function, to be minimized by parameter estimation to ensure the best possible manipulator accuracy.

In the following we briefly explain the mathematical formulation of the parameter estimation scheme implemented. The multivariable objective function ϕ depends on all 54 kinematic parameters, and may be expressed as the second-order expansion of a Taylor series as

$$\phi(p + \Delta p) \cong \phi(p) + g^T \Delta p + \frac{1}{2}\Delta p^T H \Delta p , \qquad (5)$$

where p is the 54-vector of nominal parameter values and Δp is a small perturbation of p. The 54-vector g is the gradient of the objective function ϕ with respect to p. The gradient vector represents the direction of maximum rate of change of the objective function surface and has zero magnitude at a minimum of ϕ. Matrix H is the local Hessian of the objective function ϕ. The Hessian matrix is a 54×54 symmetric quadratic matrix which contains information about the convexity of the objective function. Since our kinematic model contains redundant parameters (a total of 54 parameters as opposed to 36 independent parameters) the Hessian matrix is singular. Even in a nonredundant kinematic model, singularities may still occur if the collected data fails to excite all the parameters.

The well known *steepest descent method* (also called the *gradient search method*) selects a movement in p-space precisely opposite to the gradient vector g. The search technique continues iteratively downhill until a local minimum of the objective function ϕ is reached. Alternatively, under the *Gauss-Newton* algorithm, an iteration step is taken according to

$$\Delta p = -H^{-1} g \qquad (6)$$

which minimizes the objective function in a small neighborhood of the current objective function value. The step size varies inversely with the local curvature of the objective function. The elements of the update vector Δp are added to the corresponding elements of the parameter vector p to give an improved set of

parameters. This process continues until one or more convergence criteria are met [19].

Although the steepest descent method is guaranteed to reach a local minimum or a saddle point, the disadvantage of this method is that it often requires an excessively large number of iterations for convergence. The Gauss-Newton method, on the other hand, fails whenever the Hessian matrix is singular. It was observed by Fletcher [10] that, even in the case of positive definite Hessians, convergence may not be assured.

A robust algorithm to solve singular systems was developed independently by Levenberg [17] and Marquardt [18] and is known as the Levenberg-Marquardt algorithm [19], [20]. This algorithm has been successfully used in the parametric synthesis of kinematic linkages by Tull and Lewis [25] and Chen and Chan [3]. In recent years, it has become popular with the robotics community, especially in robot parameter estimation applications [1], [13].

In the Levenberg-Marquardt algorithm, (6) is modified as

$$\Delta p = - (H + \lambda I)^{-1} g \qquad (7)$$

where λ is an adjustable scalar and I is an identity matrix. A sufficiently large λ *is* always available which makes the inversion of $H + \lambda I$ possible. This method represents a useful combination of the steepest descent and the Gauss-Newton techniques.

The search procedure commences with a large λ and an initial guess for the model parameters. The behavior of the algorithm resembles the steepest descent method at this time. For every successful iteration, as reflected by a decrease in the objective function, λ is adjusted to a lower value. As the search progresses, successive steps increasingly resemble Gauss-Newton steps.

In order to avoid calculating the elements of H, which are second derivatives of ϕ, the gradient and the Hessian matrix may be expressed as [12]

$$g = -2J^T f \text{ and } H = 2J^T J \qquad (8)$$

where f is an n-vector of residuals and J is an $n \times 54$ Jacobian matrix (recall that n is the number of data collection points). Note that this Jacobian matrix should not be confused with the common 6×6 Jacobian matrix that maps joint displacements to endpoint displacements. Rather, an element J_{ij} of the Jacobian matrix is expressed as

$$J_{ij} = \frac{\partial f_i}{\partial p_j}, \qquad (9)$$

where f_i is the ith element of the residual vector f and p_j is the jth element of the parameter vector p.

In practice, enough calibration data should be collected (more than the minimum number necessary to solve (7), see [23]) to populate the portion of the workspace where greatest accuracy is desired. The Jacobian matrix therefore contains many more rows (equal to the number of data points) than columns (equal to the number of parameters).

Equation (7) may now be rewritten as

$$\Delta p = (J^T J + \lambda I)^{-1}(J^T f). \qquad (10)$$

Equation (10) is called the *normal equation* of this least-squares optimization. We use this equation in error minimization.

The total number of iterations required for the convergence depends on factors such as the topology of the objective function surface (its shallowness or its depth) and the closeness of the initial parameter set p to the optimal set. Since our objective function is a sum of squared errors, the topology of this surface is that of a parabolic bowl (for positive definite Hessian) or an infinite trough (for positive semidefinite Hessian). In either case, the function surface is well conditioned for the convergence.

If the initial parameter set p is far away from the optimal set, convergence is slower. For our purpose, the design parameters of the manipulator, which are supplied by the manufacturer, serve as a good initial parameter set p. In most cases convergence occurred within ten iterations.

Data Collection

Our data collection procedure involves measuring the distance of the robot endpoint from suitable fixed positions in the robot's workspace. The single scalar distance measured falls far short of the six-vector which would be required in order to fully determine the pose of the endpoint. It is useful to compare our data collection "kinematics" with that of a Stewart platform. In a Stewart platform, six linear actuators are connected between three corners of an equilateral triangular base and three corners of an equilateral triangular platform. At any configuration the actuator lengths completely determine the pose of the platform relative to the base [9]. We use three magnetic chucks mounted on a equilateral triangular fixture on the robot table and imagine the fixture as the Stewart platform base. Another fixture with three steel spheres mounted to the robot endpoint assumes the role of the platform.

If we could simultaneously use six ball-bars to couple the fixed base to the endpoint platform we could fully determine the six-dimensional endpoint pose *at every robot pose*. However we find it equally effective to "serialize" the procedure by commanding the robot to travel on a hemispherical shell (such as one shown in Fig. 2) while only one ball-bar is connected between the endpoint platform and the fixed base. We repeat this procedure six times using different pairings of base fixture magnetic chucks and endpoint platform steel spheres. We find we can in this way perform a complete parameter identification with a single ball-bar at the cost of extra time.

We use the fixture shown in Fig. 1 to mount the three steel spheres to the robot endpoint. The fixture must be such that the three spheres are not collinear. Other design concerns are low overall weight to minimize gravity loading, and small size to minimize interferences. The fixture used to mount the three magnetic chucks to the workspace is shown at the bottom of Fig. 1. The three magnetic chucks must not be collinear, and the fixture should be mounted in a location such that the hemispherical shells traced out by the ball-bar lie where the highest robot accuracy is desired.

For data collection to be automated, the ball-bar must remain connected to the robot. Unfortunately, the limited reach of the ball-bar substantially restricts the robot endpoint's positional freedom. Furthermore, interference between the ball-bar and the robot-mounted fixture must be avoided.

The net effect of these restrictions is that (as usual) the path planning cannot be done on-line using Unimation's VAL robot controller user interface. Path planning must be done off-line

using an external computer. We used an inverse kinematics routine based on the uncalibrated robot model for path planning. We define positions where we wish to collect data. These positions are located at the intersections of selected latitude and longitude lines on the hemisphere reachable by the ball-bar at the midpoint of its travel range (see Fig. 2). Moving the robot between these data points without exceeding the ball-bar range requires the use of intermediate path points ("via" points). The off-line path planning must also avoid robot joint limits and singularities. The output of path planning is a list of robot joint angle six-vectors, each corresponding to a data collection pose or a "via."

During on-line data collection, the external program transmits the list of joint vectors to the robot controller. The program commands the robot to sequentially move through the "vias," stopping at the data collection points for 2 s (to allow any dynamic oscillations to subside), before reading the ball-bar length and the current robot joint angles (which may differ slightly from the commanded joint angles). This information is then recorded for later use in an off-line parameter identification program described below.

As mentioned, a minimum of six trajectories on six hemispherical shells must be used to collect data. Since collection of excess data is always beneficial, sometime we used all nine possible ball-bar connections. Also, we used ball-bar extension rods to collect additional sets of data on hemispherical shells with larger radii.

Pose Measurements:
How Many Dimensions Are Enough?

Duelen and Schroer [5] state that all of the kinematic parameters of a manipulator may be identified by measuring only the position of a suitable point on the end-effector. The only requirement is that the measurement point should not be on the axis of the robot's last joint. In our experiment, however, we were able to identify only 33 parameters while measuring the distance of a single endpoint-mounted steel sphere from all three fixed chucks. Measurement of the three distances is equivalent to measuring the three Cartesian position coordinates of the steel sphere which, in fact, is not on the robot's sixth joint axis. The three orientation parameters of the last link elude identification in this case. A recent paper also supports our results [29]. If the endpoint-mounted steel sphere happens to lie on the sixth joint axis we fail to identify, additionally, the error in the sixth joint offset.

In order to evaluate the possible physical changes in any of the link geometric features or joint encoders characteristics, the collected data must "excite" all 36 independent parameters of the PUMA 560 robot. The number of excited (or identified) parameters is given by the number of linearly independent columns in the Hessian matrix H or the Jacobian matrix J. Counting the number of nonzero singular values of H or J therefore constitutes a simple test for calculating the number of identified parameters [12], [29].

We ran several parameter identification trials with different subsets of the nine possible endpoint platform/fixed-base pairings. The number of identified parameters for each case is shown in Table I. The results indicate that by using all nine pairings, we can identify the complete set of 36 independent kinematic parameters. In fact any six of these nine pairings are sufficient, so long as no steel sphere or magnetic chuck is uninvolved.

It is notable that we do not need to (and in practice we do not) cause the robot endpoint to adopt the *same* set of poses for each base-platform pairing. Because of this, no single pose can ever be fully determined (six-dimensionally) from the data collected, but as far as parameter identification is concerned it as if full six-dimensional endpoint poses were determined.

Results and Discussion

In order to check the success of the parameter estimation process, we collected radial distance data for two distinct sets of hemispherical shells. The radius of the first set was 46 cm, and the radius of the second set was 61 cm, obtained by using a 15-cm extension of the ball-bar. Each set consisted of about 800 poses. We computed the optimal parameters for the 46 cm radius set of shells and used the new parameters to compute error residuals for the second set of shells (61 cm).

The RMS residual radial length error for the 46 cm set of shells was found to be 0.084 mm. Since the same data was used for optimization as for error evaluation, there is an element of "mindless curve fitting" involved. Indeed, if we had measured only 36 poses we could obtain a residual error of zero no matter how poor the result would be on additional poses or on poses in another part of the workspace.

Table I
Different Ball-Bar Pairings and
the Number of Identified Parameters

Number of magnetic chucks on robot table	Number of spherical balls on robot endpoint		
	1	2	3
1	30	32	33
2	32	34	35
3	33	35	36

To avoid both "mindless curve fitting" and also to test whether the optimized parameters work well outside the calibrated workspace, we computed error residuals for the 61-cm shells using the robot parameters determined for the 46-cm shell. The residual error was only 0.110 mm. This result implies that the optimized kinematic model correctly reflects the robot geometry, and is not simply a best fit of the data used for calibration.

Fig. 3, which shows a distribution of the final residuals on the longitudes of the data collection hemispherical shell (see Fig. 2), demonstrates that the residuals do not vary significantly with spatial position and thus, they reflect random errors such as repeatability and gear backlash rather than the errors in the geometric parameters.

In Fig. 4 we plot a histogram of the final residuals. The Gaussian distribution curve which fits the histogram has a mean of 0.0 mm and a standard deviation of 0.084 mm has been
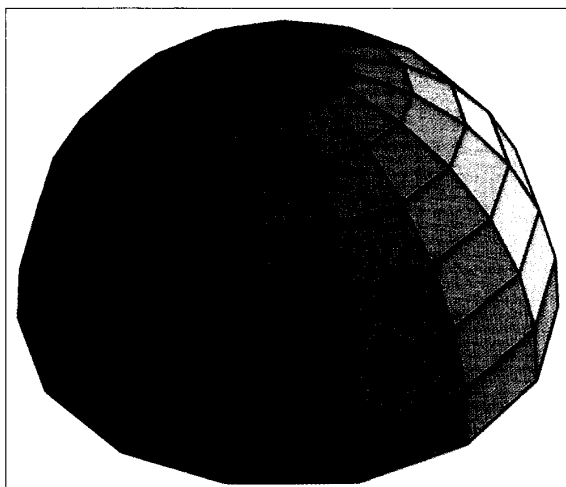
Fig. 2. An imaginary hemispherical shell on which the robot is programmed to travel. Measurement takes place on each indicated data collection point.

superimposed on the histogram. The final residuals are seen to be normally distributed about zero error.

In Table II, we list the design kinematic parameters (manufacturer supplied) of a PUMA 560 manipulator and the optimized kinematic parameters we obtained. We selected a set of 36 independent parameters and held the remaining 18 parameters fixed arbitrarily at their design values. We caution that a direct comparison between a design parameter and its optimized value is not very meaningful for several reasons. The first six parameters describe the robot's first link which incorporates not only the robot base, but also our magnetic chuck fixture which was placed, somewhat arbitrarily, within a few centimeters of its intended position on the robot's worktable. Our global coordinate frame was defined by one of the chucks of the fixture. This means that even if the parameters of the robot's first link are perfectly known, the mounting position of the magnetic chuck fixture will cause their optimized values to be different from their design values. In other words, there is no way to distinguish between the actual link parameter errors and the mounting errors, for the first link.
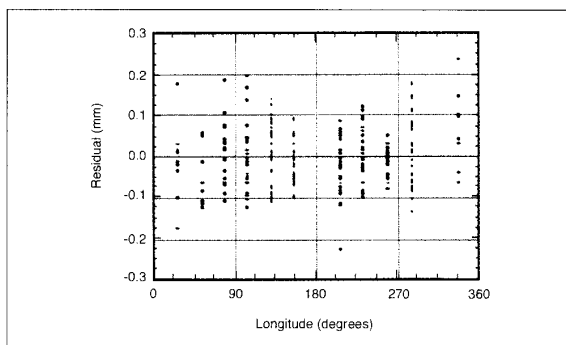

Fig. 3. Plot of the distribution of the final residuals versus longitude of the hemispherical calibration shell.

A second caveat arises due to the redundancy of our kinematic model. Since we are forcing certain parameters (18 of them in total) to remain fixed, any errors in the corresponding physical dimensions will be accommodated by one or more of the other 36 parameters. Therefore, a difference in the design value and the optimized value of a certain parameter may not necessarily mean an actual change of the corresponding physical feature, and could equally well be due a combined error in several other physical features.

Finally, casual readers should be warned that the optimized parameters displayed here result in improved accuracy for our robot, with its particular manufacturing tolerances, wear, joint encoder offset angles, etc. These parameters would not improve the performance of another robot of the same model.

It is important to distinguish between the RMS error of radial distances and the RMS error of the robot endpoint Cartesian position. We estimated numerically the positional error of the endpoint for a given RMS error of the radial distance. The Stewart platform analogy is again useful here. Imagine that the robot endpoint triangle (with three steel spheres) and the base triangle (with three magnetic chucks) are interconnected through six ball-bars in a Stewart platform geometry. The question we then ask is: for 0.084-mm RMS errors in the ball-bars, what is the RMS error in the positioning of the triangle?

The Jacobian matrix of a Stewart platform transforms small changes in its leg lengths to small changes in the pose of the platform [9]. For a nominal configuration of our imaginary Stewart platform (the robot endpoint plate situated directly over the base triangle with all the ball-bars of equal length) we computed how errors in each of its leg lengths propagate to motions of the top platform. Using an RMS error of 0.084 mm in leg length we find the Cartesian positional error to be roughly four times the ball-bar error, or 0.34 mm.

Easy and Economic Procedure

We have shown that partial pose information can be used to identify all the independent kinematic parameters of a robot. We used a simple radial-distance transducer (an LVDT) to measure the distance of the robot endpoint from fixed points in the
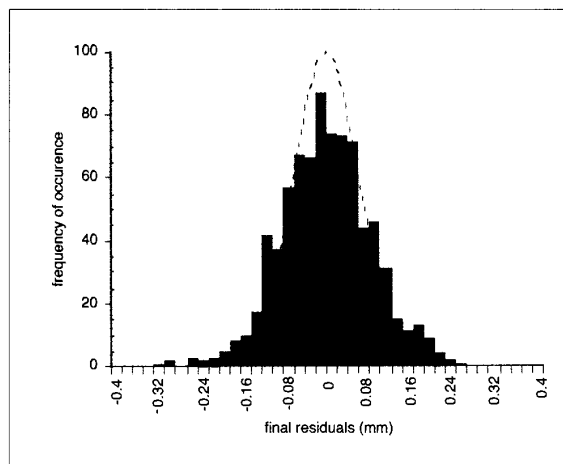

Fig. 4. Histogram of the final residuals from 800 calibration points.

		Parameters as supplied by the manufacturer	Optimized kinematic parameters	
x_1	cm	0	1.25885	depends on mounting
y_1	cm	0	-0.192122	depends on mounting
z_1	cm	66.04	66.8858	depends on mounting
α_1	°	0	0.0750332	depends on mounting
β_1	°	0	0.0563741	depends on mounting
γ_1	°	0	0.142109	depends on mounting
jt encoder offset 1	°	-90	-90	held fixed (#1)
jt encoder factor 1		1	0.999217	
x_2	cm	-18	-18.0803	
y_2	cm	0	0.0706535	
z_2	cm	0	0	held fixed (#2)
α_2	°	90	90	held fixed (#3)
β_2	°	0	-0.277037	
γ_2	°	-90	-90.0001	
jt encoder offset 2	°	0	0	held fixed (#4)
jt encoder factor 2		1	1.0008	
x_3	cm	43.18	43.3215	
y_3	cm	0	0.639884	
z_3	cm	-3.091	-3.091	held fixed (#5)
α_3	°	0	0	held fixed (#6)
β_3	°	0	-0.137778	
γ_3	°	0	-0.116512	
jt encoder offset 3	°	-90	-90	held fixed (#7)
jt encoder factor 3		1	1.00005	
x_4	cm	43.307	43.3068	
y_4	cm	-2.032	-2.12003	
z_4	cm	0	0	held fixed (#8)
α_4	°	90	90	held fixed (#9)
β_4	°	0	-0.0246447	
γ_4	°	90	90.0979	
jt encoder offset 4	°	0	0	held fixed (#10)
jt encoder factor 4		1	0.998821	
x_5	cm	0	-0.0109964	
y_5	cm	0	-0.0434906	
z_5	cm	0	0	held fixed (#11)
α_5	°	0	0	held fixed (#12)
β_5	°	0	-0.496135	

Table II
Design Kinematic Parameters
and Optimized Values for a PUMA 560 Manipulator

		Parameters as supplied by the manufacturer	Optimized kinematic parameters	
γ_5	°	-90	-90.0111	
jt encoder offset 5	°	0	0	held fixed (#13)
jt encoder factor 5		1	1.00053	
x_6	cm	0	0.00523043	
y_6	cm	0	0.0394295	
z_6	cm	0	0	held fixed (#14)
α_6	°	0	0	held fixed (#15)
β_6	°	0	3.18249	
γ_6	°	90	89.9855	
jt encoder offset 6	°	0	0	held fixed (#16)
jt encoder factor 6		1	1.00016	
x_7	cm	0	0.00166565	
y_7	cm	0	-0.00298551	
z_7	cm	5.625	5.625	held fixed (#17)
α_7	°	0	0	held fixed (#18)
β_7	°	0	-0.0185442	
γ_7	°	0	-0.00889793	

Table II (continued)

workspace. Our procedure represents an easy and economic way of calibrating a robot.

References

[1] J.R. Bosnik, "Static and vibrational kinematic parameter estimation for calibration of robotic manipulators," Ph.D. thesis, Pennsylvania State Univ., University Park, PA, 1986.

[2] P.L. Broderick and R.J. Cipra, "A method for determining and correction of robot position and orientation errors due to manufacturing," *ASME J. Mechanisms, Transmissions, and Automation in Design*, vol. 110, pp. 3–10, 1988.

[3] F.Y. Chen and V.-L. Chan, "Dimensional synthesis of mechanisms for function generation using Marquardt's compromise," *ASME J. Eng. Ind.*, vol. 96, no. 1, pp. 1312–1317, 1974.

[4] J. Chen and L. M. Chao, "Positioning error analysis for robot manipulators with all rotary joints," in *Proc. IEEE Int. Conf. Robotics Auto.*, 1986, pp. 1011–1016.

[5] G. Duelen and K. Schroer, "Robot calibration—method and results," *Robotics Computer-Int. Manufact.*, vol. 8, no. 4, pp. 223–231, 1991.

[6] L.J. Everett, M. Driels, and B.W. Mooring, "Kinematic modelling for robot calibration," in *Proc. IEEE Int. Conf. Robotics Auto.*, 1987, pp. 183–189.

[7] L.J. Everett and T.-W. Hsu, "The theory of kinematic parameter identification for industrial robots," *ASME J. Dynamic Syst., Meas., and Control*, vol. 110, pp. 96–100, Mar. 1988.

[8] L.J. Everett and A.H. Suryohadiprojo, "A study of kinematic models for forward calibration of manipulators," in *Proc. IEEE Int. Conf. Robotics Auto.*, Philadelphia, PA, 1988, pp. 798–800.

[9] E.F. Fichter, "A Stewart platform based manipulator: General theory and practical construction," *Int. J. Robot. Res.*, vol. 5, no. 2, pp. 157–182, 1986.

[10] R. Fletcher, *Practical Methods of Optimization*. New York: Wiley, 1980.

[11] K.S. Fu, R.C. Gonzalez, and C.S.G. Lee, *Robotics: Control, Sensing, Vision, and Intelligence*. New York: McGraw-Hill, 1987.

[12] A. Goswami and J.R. Bosnik, "On a relationship between the physical features of robotic manipulators and the kinematic parameters produced by numerical calibration," *ASME J. Mech. Des.*, 1993.

[13] J.M. Hollerbach, "A survey of kinematic calibration," *Robot. Rev.* Cambridge, MA: M.I.T. Press, 1989.

[14] R.P. Judd and A.B. Knasinski, "A technique to calibrate industrial robots with experimental verification," in *Proc. IEEE Int. Conf. Robot. Auto.*, 1987, pp. 351–357.

[15] T.C. Kienzle, S.D. Stulberg, M. Peshkin, A. Quaid, and C.-H. Wu, "An integrated CAD-robotics system for total knee replacement surgery," in *Proc. IEEE Conf. Syst., Man, Cybern.*, Chicago, IL, 1992.

[16] K. Lau, N. Dagalakis, and D. Myers, "Testing," in *Int. Encyclopedia Robotics: Appl. Auto.*, New York: Wiley, 1984.

[17] K. Levenberg, "A method for the solution of certain non-linear problems in least-squares," *Quart. Appl. Math.-Notes*, vol. 2, no. 2, pp. 164–168, 1944.

[18] D.W. Marquardt, "An algorithm for least-squares estimation of nonlinear parameters," *J. Soc. Ind. Appl. Math.* vol. 11, no. 2, pp. 431–441, 1963.

[19] J.C. Nash, *Compact Numerical Methods for Computers: Linear Algebra and Function Minimization.* New York: Wiley, 1979.

[20] W.H. Press, B.P. Flannery, S.A. Teukolsky and W.T. Vetterling, *Numerical Recipes, The Art of Scientific Computing.* Cambridge, U.K.: Cambridge Univ. Press, 1985.

[21] Z. Roth, B.W. Mooring, and B. Ravani, "An overview of robot calibration," *IEEE Trans. Robot. Auto.*, vol. 3, no. 5, pp. 377–385, 1987.

[22] P.N. Sheth and J.J. Uicker, "A generalized symbolic notation for mechanisms," *ASME J. Eng. Ind.,* vol. 93, no. 1, pp. 102–112, 1971.

[23] H.J. Sommer and N.R. Miller, "A technique for the calibration of instrumented spatial linkages used for biomechanical kinematic measurements," *J. Biomechanics*, vol. 14, no. 2, pp. 91–98, 1981.

[24] H.W. Stone, *Kinematic Modeling, Identification, and Control of Robotic Manipulators.* Norwell, MA: Kluwer, 1987.

[25] H.G. Tull and D.W. Lewis, "Three dimensional kinematic synthesis," *ASME J. Eng. Ind.,* vol. 90, no. 3, pp. 481–484, 1968.

[26] K. Vira and K. Lau, "Design and testing of an extensible ball bar for measuring the positioning accuracy and repeatibility of industrial robots," in *Proc. NAMRAC Conf.*, 1986, pp. 583–590.

[27] C.H. Wu, J. Papaiannou, T. C. Kienzle, and S. D. Stulberg, "A CAD-based human interface for preoperative planning of total knee surgery," *IEEE Conf. Syst., Man, Cybern.,* Chicago, IL, 1992.

[28] J. Zeigert and P. Datseris, "Basic considerations for robot calibration," in *Proc. IEEE Int. Conf. Robot. Auto.*, Philadelphia, PA, 1988, pp. 932–938.
[29] H. Zhuang, Z.S. Roth, and F. Hamano, "Observability issues in kinematic identification of manipulators," *ASME J. Dynamic Syst., Meas., Control*, vol.114, pp. 319–322, June 1992.

Ambarish Goswami received the Bachelor's degree from Jadavpur University, Calcutta, India, and the Master's degree from Drexel University, both in mechanical engineering. He obtained the Ph.D.degree under the direction of Michael Peshkin at Northwestern University in 1993. Currently he is doing post-doctoral research at INRIA Lab in Grenoble, France. His current research interests are in robot calibration, force guided assembly, programmable passive mechanical devices, computer-assisted surgery, and biped robots. He is a member of IEEE and ASME.

Arthur Quaid received the B.S. degree in mechanical engineering in 1993 from Northwestern University, Evanston, IL. As an undergraduate, he worked on robot calibration and the development of a robot-assisted total knee replacement surgery system and he coauthored several journal articles, conference papers, and book contributions in these areas. He is now working towards the Ph.D. degree in robotics at Carnegie Mellon University's Robotics Institute in Pittsburgh, PA. He is a member of IEEE and ASME.

Michael Peshkin received the Bachelor's degree from the University of Chicago, the Master's degree from Cornell University, and the Ph.D. degree from Carnegie-Mellon University in 1986, all in physics. At Carnegie-Mellon he worked in the University's Robotics Insitute under the direction of Arthur Sanderson. He is now an Associate Professor of Mechanical Engineering at Northwestern University. Current research interests in robotics are task planning, force guided assembly, programmable passive devices, and computer assisted surgery. Other interests include neural networks and the evolution of random cellular networks. He was an NSF Presidential Young Investigator in 1988, and is the author of 36 technical publications. He is a member of IEEE, ASME, and APS.